Science of the Total Environment 908 (2024) 168144

Contents lists available at ScienceDirect

Science of the Total Environment

journal homepage: www.elsevier.com/locate/scitotenv

A rapid and portable fluorescence spectroscopy staining method for the detection of plastic microfibers in water

Devlina Das Pramanik [a,b,*], Paul Kay [c], Francisco M. Goycoolea [a]

[a] School of Food Science and Nutrition, University of Leeds, LS2 9JT, United Kingdom
[b] Centre for Biotechnology and Biochemical Engineering, Amity Institute of Biotechnology, Amity University, Noida, Uttar Pradesh 201301, India
[c] School of Geography, University of Leeds, LS2 9JT, United Kingdom

HIGHLIGHTS

- A hydrophilic and anionic dye was used for the detection of synthetic microfibers.
- A portable photometer (Lovibond MD-640) was employed for the microfiber detection.
- Detection was performed on microfiber spiked fresh, estuarine & sea water samples.
- The bound dye was recovered using xanthan gum as a competing anionic moiety.
- Recovered dye was subjected to sunlight mediated degradation.

GRAPHICAL ABSTRACT

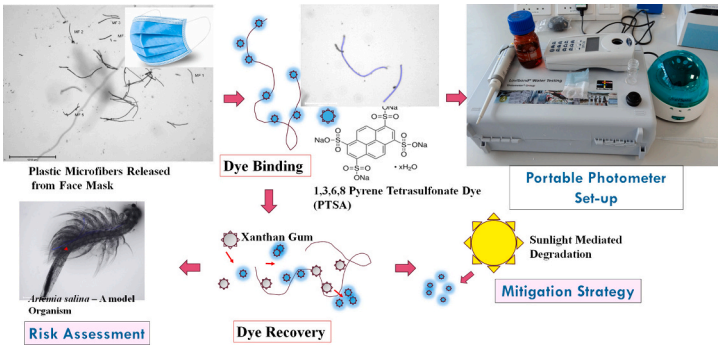

ARTICLE INFO

Editor: Yi Yang

Keywords:
1,3,6,8 Pyrene Tetrasulfonate (PTSA)
Fluorescence-based detection
Microfibers
Portable photometer

ABSTRACT

We propose a simple technique for microplastic detection based on their interaction with a hydrophilic and anionic fluorescent dye 1,3,6,8 pyrene tetrasulfonate (PTSA). Synthetic microfibers derived from surgical face masks (an abundantly generated plastic waste post COVID) were considered as model microplastics. The interactions between microfibers and the dye were studied as a function of physiological parameters (pH, contact time and temperature), external agents, dye dosage and polymer variants. A pocket-sized photometer (by Lovibond Tintometer group) was employed for the detection and further validated using advanced equipment set-ups (fluorescence microscope, Fourier transform infrared spectroscopy and benchtop spectrofluorometer). Risk assessment studies were conducted on *Artemia salina* as a model organism. As a risk mitigation strategy, dye recovery followed by sunlight mediated degradation were performed. The detection study was performed in real water samples collected from fresh, estuarine and seawater samples spiked with microfibers. As an outcome, an optimized standard operational conditions were determined for the effective detection of synthetic microfibers. The data obtained could have scientific and industrial impact, in particular for experts working in the broad arena of clean water, who are specifically interested in developing cost-effective solutions for effective detection and biomonitoring of emerging pollutants.

* Corresponding author at: School of Food Science and Nutrition, University of Leeds, LS2 9JT, United Kingdom.
E-mail address: d.pramanikleeds@gmail.com (D.D. Pramanik).

https://doi.org/10.1016/j.scitotenv.2023.168144
Received 7 September 2023; Received in revised form 11 October 2023; Accepted 24 October 2023
Available online 7 November 2023

1. Introduction

Poor plastic management techniques have boosted the persistence of microplastics in the environment (Brown et al., 2023). During the ongoing and post-COVID period, disposable face masks have been extensively used resulting in the generation and release of humongous amounts of microfibers, as a common form of microplastics (Anastopoulos and Pashalidis, 2021). Microfibers released from face masks have been recognized as an emerging pollutant and are currently receiving global attention owing to their widespread nature and potential adverse impacts (Cabrejos-Cardeña et al., 2023). A detailed analysis performed by researchers from the University of Portsmouth, UK showed a constant increase in the usage of face masks as compared to wipes and gloves during the period May 2020 to October 2020. Evidence of microplastic (microfibers in particular) leaching from face masks continues to accumulate (Chen et al., 2021; Idowu et al., 2023). Thus, for our study, we have employed surgical face masks as a starting material and the obtained synthetic microfibers as a model microplastic material. Being an emerging pollutant, it is vital to study the distribution via improved qualitative and quantitative detection techniques/tools. Fluorescent staining techniques could help identify and detect microplastics (Table 1). Nile red, a fluorescent dye is commonly used for microplastic detection via fluorescence microscopy technology (Shim et al., 2016). Although the dye ensures a strong fluorescence signal and fast staining rate, however, some of the challenges associated with the use of Nile Red are associated with its solubility in an aqueous environment, specifically to detect the microfibers evenly suspended in water and the involvement of solvents such as DMSO and di-methyl formamide which could pose toxicity risks while performing the assays onsite. Also, a high-resolution fluorescence microscope along with a benchtop spectrofluorometer would be essential to assess the changes in fluorescence. There is an unmet need to further investigate enabling the applicability of portable photometers towards microplastic detection. In this regard, it would be worthy to mention the contribution of the team of Asamoah et al, who developed and designed a prototype of a portable optical sensor for the detection of transparent and translucent microplastics in a freshwater environment (Asamoah et al., 2021). The proposed research is the first study employing the dye PTSA for microplastic detection via a portable photometer. The team of Asamoah developed a portable prototype optical sensor for the detection of transparent and translucent microplastics in water. The detection was based on the simultaneous recording of the specular light reflection signal and the forward interference pattern from the light-microplastic interactions in water (Asamoah et al., 2019). However, there is an unmet need to conduct a thorough analytical study on the applicability of portable devices for microplastic detection.

In the proposed research we have employed a different scientific approach for microplastic detection based on estimating the changes in fluorescent intensities. A detailed study has been performed on microfiber detection using a portable photometer MD-640 (by the Lovibond Tintometer group). As already programmed in the photometer set-up, 1,3,6,8 pyrene tetra sulfonate (PTSA) dye has been used as a fluorescent dye to stain the microfibers. A recent study on microplastic detection by fluorescent staining method has been reported by the team of Lv et al., 2019. The research group developed a methodology to detect microplastics using the dyes Safranin, FITC, and Nile Red. The scientific hypothesis of the dye binding was justified based on thermal expansion and contraction properties. However, the instrumentation for detection involved light microscopy, Raman spectroscopy, and scanning electron microscopy (Lv et al., 2019). The research work justifies the hypothesis of microplastic detection using fluorescence-based detection, however, it necessitates improvisation so as to enable the applicability of portable photometer. Our proposed research involved PTSA is a hydrophilic and anionic fluorescent dye with excellent fluorescence properties (Jiao et al., 2020). Research on developing applicability using PTSA has drawn considerable interest for imaging and labelling, both industrial

Table 1
Recent reports on microplastic detection using fluorescent dyes.

S. No.	Fluorescent dye used	Polymeric nature of microplastics	Brief outcome	Reference
1.	Nile Red	Polystyrene, Polyethylene, Polyacrylonitrile, Polycarbonate, Polyethylene terephthalate, Polypropylene, polyurethane, Polyvinyl chloride	Microfibers from tap and bottled water samples were identified using reactive Nile Red. Difference in manifestations of fluorescence was noted when environmental microfiber samples were compared with pristine polymers.	Alvim et al., 2023
2.	Nile Red	Polystyrene in abundance	A comparative profiling of the number, size, shape, and polymer type of microplastics was done using micro-FTIR imaging and Nile red staining.	de Guzman et al., 2022
3.	2,5-Bis(5-tert-butyl-2-benzoxazolyl) thiophene and Nile red	Polypropylene	An in-situ selective fluorescent illumination of the MPs in water was attempted with the aid of surfactant.	(Park et al., 2022)
3.	Nile Red	Polyethylene, Polyethylene terephthalate, Polypropylene, Polystyrene and Polyvinyl chloride	A cost- and time-effective, automated method to identify microplastics was reported. Two machine learning models that used RGB color quantification were proposed which combined image analysis of fluorescent particles with classification models.	(Meyers et al., 2022)
4.	Nile Red	Polystyrene, Polypropylene, Polyethylene, Polyamide	The efficacy of Nile red towards microplastic detection was evaluated by a systematic investigation of the variations in particle pixel brightness (PPB).	(Nel et al., 2021)
5.	Nile Red	Polyethylene, Polyethylene Terephthalate, Polystyrene, Polypropylene	A combination of Nile Red staining and micro-Raman spectroscopy was used for the identification of microplastics.	(Prata et al., 2021)
6.	Nile Red	Low density polyethylene	The limitations of using Nile Red in biota were investigated using marine mussels as model organisms.	(Nalbone et al., 2021)

(*continued on next page*)

Table 1 (*continued*)

S. No.	Fluorescent dye used	Polymeric nature of microplastics	Brief outcome	Reference
7.	Nile Red	Polyester urethane, Vinyl chloride/ Vinyl acetate Copolymer, Plasticized PVC, Poly(*p*-phenylene ether sulfone), Vinyl chloride/Vinyl acetate copolymer, Polyethylene terepthalate, Acrylonitrile/ butadiene/styrene copolymer, Butadiene/styrene copolymer, Poly (N-vinyl carbazole), Polyethylene terepthalate, PVC/ Acrylic alloy, and Poly(ethylene-*co*-vinyl acetate)	Microplastic detection was carried out using Nile Red on two bivalve species (*Perna viridis* and *Meretrix meretrix)* collected from three estuaries.	(Dowarah et al., 2020)
8.	Safranine T, Fluorescein isophosphate and Nile red	Polyethylene, Polystyrene, Polyvinyl Chloride and Polyethylene Terephthalate	An improved fluorescent staining method for detection and quantification of microplastics was developed based on thermal expansion and contraction.	(Lv et al., 2019)
9.	1,3,6,8 pyrene tetra sulfonate (PTSA)	Microfibers leached from surgical face masks Pristine Standards: Polyethylene, Polypropylene, Cellulose and Polyester	The present study employs 1,3,6,8 pyrene tetrasulfonate as an anionic hydrophilic dye for the detection of synthetic microfibers using a commercially used pocket photometer (MD-640, Lovibond Tintometer group).	Our Study

and biomedical applications. PTSA has been applied in industrial coolants for monitoring changes in corrosion. Currently, published scientific reports on PTSA have focused on their applicability as an anti-counterfeit agent (Jiao et al., 2020; Chen et al., 2019). In the year 2020, the team of Jiao et al. reported a strategy to improve the luminescent properties of the hydrophilic dye by doping it into silica nanoparticles using cationic polyelectrolyte poly (dimethyl diallyl ammonium chloride; PDADMAC) as a bridge. However, the applicability of PTSA for environmental monitoring and specifically the detection of emerging microplastics pollutants has not been well explored.

The present study reports the applicability of PTSA dye in the detection of synthetic microfibers in an aqueous environment. As an innovative approach, we have employed MD-640, a portable photometer (by Lovibond® Tintometer group) as a portable apparatus to quantify the changes in fluorescence intensities post-binding with both natural and synthetic polymeric microfibers. We have explored the interactions between dye with the microfibers under different physiological conditions, polymeric variants, external agents, dye dosage and microfiber count. The readouts obtained from the portable photometer has been validated using fluorescence emission spectra (obtained using a benchtop spectrofluorometer) and a fluorescence microscope. Risk assessment has been a vital parameter which has been explored. A brine shrimp *Artemia salina* (a zooplankton) was employed as a model organism for toxicity studies. A two-step mitigation strategy has been developed which involves dye recovery followed by sunlight mediated degradation. The as-developed standardized protocol in the lab was further employed to detect spiked synthetic microfibers in three different real water samples collected from freshwater, estuarine water and seawater bodies in the Yorkshire region, UK.

2. Materials and methods

Chemicals used for our study and a discussion on the methodology for preliminary characterization of microfibers have been included in the Supplementary Sections 1.1 and 1.2 respectively.

2.1. PTSA binding studies

Microfibers were characterized using microscopy, spectroscopy and thermogravimetry techniques (discussed in detail under Supplementary Sections 1.2 and 2.2; Figures: S1(a)-(m); S2(a)-(e); S3; S4(a)-(b)). The properties of the aqueous media used in the study have been characterized and tabulated in Table S1. A 25 mL pre-counted microfiber suspension was prepared in AFW aqueous media (discussed in detail in Supplementary Section 1.2). Pre-counting of the microfibers was done using an EVOS Auto FL2 microscope at 2× magnification. A dye volume of 125 μL (equivalent to 0.6 nmoles of PTSA) was added to the microfiber suspension. At the same dye dosage mentioned above, the PTSA binding to microfibers was subjected to variations in three environmental parameters, namely, pH (4.1–9.1), temperature (4 °C–80 °C) and contact time (2 h–48 h). The effect of polymer variants and microfiber dosage on PTSA binding was also investigated.

FT-IR spectroscopy (Perkin Elmer with diamond ATR attachment) was employed for microfiber characterization and assessment of dye-microfiber interaction. Sample preparation involved interaction of 50 mg of microfibers with PTSA dye (0.6 nmoles) in an aqueous environment, followed by microfiber recovery using filtration and air-drying (for excess water removal). The PTSA binding was also assessed in the presence of external agents (water soluble: zinc chloride, sodium chloride; water-insoluble: chitin and sand, each dosed at 4 g/L). Prior to analyses, the emission peaks were noted as different excitation wavelengths (Supplementary Fig. S5). A detailed calibration was performed using different dye dosages ranging from 0 to 0.6 nmoles (S6(a)-(b)). Respective dye concentrations were obtained from an initial stock of 0.102 μmole, prepared by dissolving 5.22 mg of PTSA in 80 mL of AFW aqueous medium.

2.2. Toxicity studies on Artemia salina - a model invertebrate model

Adult brine shrimps (*Artemia salina*) were exposed to three treatment groups namely: group A (*Artemia salina* exposed to microfibers), group B (*Artemia salina* exposed to 0.512 nanomole PTSA), and group C (*Artemia salina* exposed to PTSA bound microfibers). The toxicity was assessed in terms of changes in survival (Kaplan-Meier) and swimming competencies following our previously established protocol (Das Pramanik et al., 2023). Experimentation was divided into (i) acclimatization and (ii) exposure studies (details have been discussed in Supplementary Sections 1.3.1 and 1.3.2).

2.3. Dye recovery

Experiments on PTSA recovery were performed using xanthan gum (an anionic biopolymer) as a competing moiety. Prior to dye recovery experiments, a preliminary study was conducted on two different biopolymers, namely, sodium alginate and xanthan gum, to assess the changes in the fluorescence intensities post-interaction with PTSA. A detailed description of the methodology is provided in the Supplementary Information (Section 1.4).

Post-recovery, PTSA dye samples as released from microfibers from the dye recovery experiments were subjected to degradation by natural sunlight exposure (Supplementary Section 1.5).

2.4. Statistical analyses

Statistical analyses were performed to draw effective comparisons between the obtained for various groups/sets. The models tested include a one-way ANOVA, two-way ANOVA, and *t*-test. A software tool GraphPad Prism version 9.0 was employed for the statistical analyses.

3. Results and discussion

3.1. Microfiber-PTSA interaction-FT-IR analyses

The interactions between microfibers and PTSA were assessed in terms of changes in fluorescence intensities of the resulting emission peaks, photometer readings, and merged brightfield-fluorescence images. As shown in Fig. 1(a)-(e), FT-IR analyses confirmed the specificity of the polymers towards PTSA via relevant changes in transmittance (%) values and peak shifts. Post interaction with PTSA changes in transmittance values were noted at wavenumbers 2908 cm^{-1}, 2838 cm^{-1} (due to CH_2 and -CH stretching vibrations), 1471 cm^{-1}, 1091 cm^{-1} (due to symmetric and asymmetric stretching vibrations of S═O present in -SO_3H). Similar peak stretches were noted in the case of polyethylene. However, in the case of polypropylene, the changes in transmittance at wavenumbers 2919 cm^{-1} and 2854 cm^{-1} justified the obvious involvement of alkyl groups in PTSA binding.

3.2. Effect of environmental parameters

The effect of different parameters was studied to assess the changes in fluorescence intensities resulting from quenching of PTSA dye by synthetic microfibers. The parameters studied were pH, contact time, and temperature.

Among various physiological parameters, pH is a vital parameter to be considered when studying a process. Three different pH values namely, 4.1 (acidic), pH 7.2 (neutral), and pH 9.1 (basic) were considered for the present study. As shown in the emission spectra and graphs, the levels of quenching were not significantly affected by changes in pH values (Fig. S7(a)-(b)). Merged fluorescence images revealed PTSA binding at a wide pH range (Fig. S7(c)-(e)). However, from the graphical interpretation it was observed that, at a pH value of 7.2, PTSA intensity (without microfibers) was slightly higher as compared to that of acidic pH and basic pH values. This could be attributed to the hindering activity of the surrounding protons and hydroxyl moieties. However, shifts in pH did not affect the PTSA quenching by the microfibers in any significant way. The results indicated that further quenching and microplastic detection studies could be conducted under a neutral pH environment, thereby justifying the applicability of the technology for the detection of microplastics in real environments.

The effect of different temperature set points (4 °C, 20 °C, 60 °C and

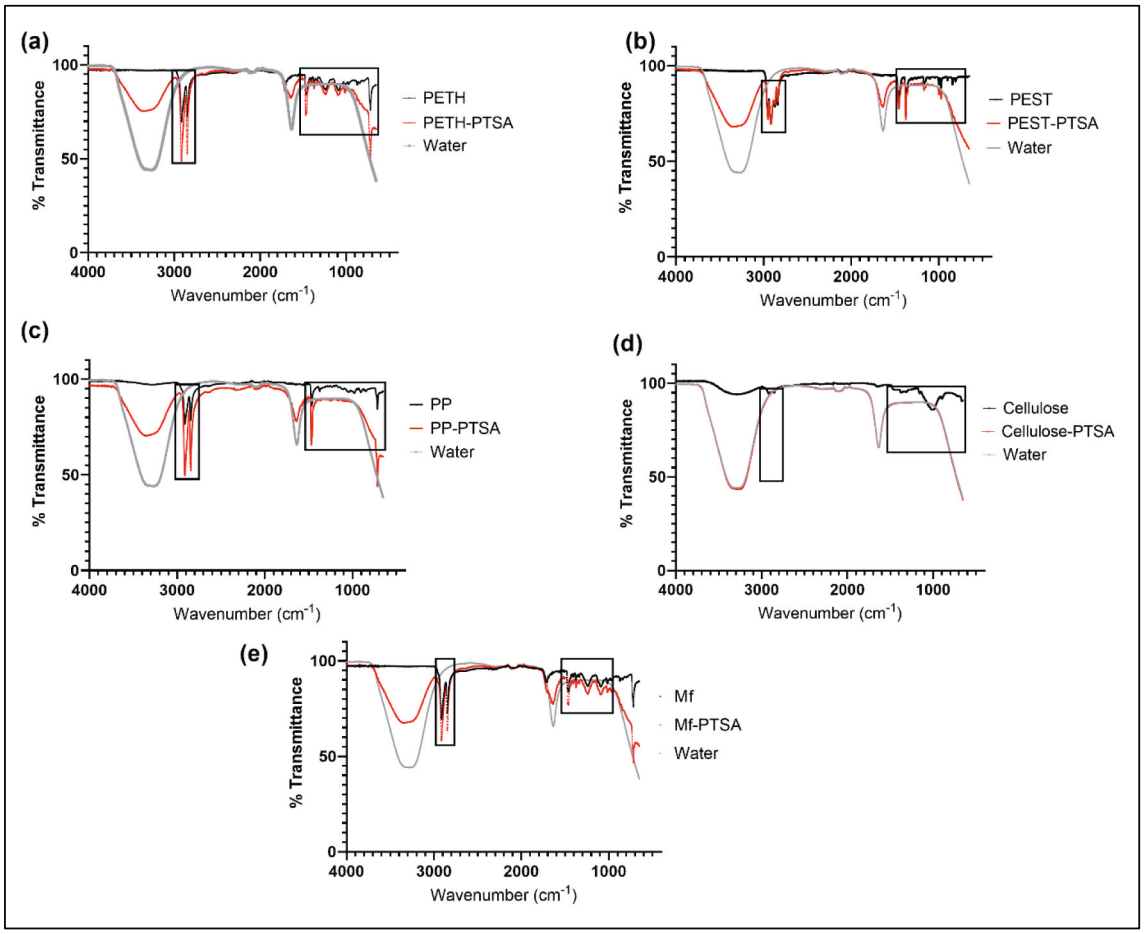

Fig. 1. FT-IR spectra of sample and standard microfibers treated with the dye PTSA*
*PTSA concentration was maintained at 0.5 nanomoles (245.7 ± 6.5 ppb). The microfiber dosage was maintained at 11 ± 2 fibers/mL.
*The acronyms can be written as follows: PP- Polypropylene; PETH- Polyethylene; PEST- Polyester; Mf- Sample Microfibers
*For obtaining the FT-IR spectra, the microfibers were in a wet state due to interaction with PTSA in an aqueous environment. The grey peaks represent that of water. The wet weight of the microfiber samples were noted as 350 mg.

80 °C) on PTSA binding by microfibers were studied. Fluorescence intensities were represented in Fig. S8(a)-(b). It was noted that the fluorescence intensities of the dye did not exhibit significant changes as a function of different temperature values of 4 °C, 20 °C, and 60 °C. However, a further increase in temperature (80 °C) resulted in a decrease in the fluorescence intensity of the dye. Similar to our results, the team of Jiao et al., 2020 reported a decrease in fluorescence brightness with an increase in temperature (up to 60 °C). This could be attributed to changes in the structural stability of the dye molecules due to the increase in collision frequency and deactivation probability (Jiao et al., 2020). Maximum fluorescence quenching was noted at a temperature of 60 °C. However, it was interesting to note that fluorescence quenching and PTSA binding could still be observed at a temperature of 20 °C. We could thus infer that a range of 20 °C–60 °C was optimum for PTSA-based detection of microplastics (Fig. S8(a)(b)(d)(e)). Low and high temperatures affected PTSA binding onto the microfibers (Fig. S8 (c), (f)).

The effect of contact time on PTSA quenching by microfibers was investigated over a period of 0.5 h – 3.5 h. The data on PTSA fluorescence intensities was obtained at every 0.5 h interval (Fig. 2(a)-(b)). As shown in Fig. 2(b), a significant difference in PTSA quenching from an interaction period of 2 h onwards. No further increase in PTSA quenching was noted beyond 2.5 h. However, beyond, 2.5 h, an increase in PTSA concentration in the surrounding solution was noted, which could be attributed to PTSA leaching from the microfibers back into the surrounding AFW aqueous environment. Bright-field-fluorescence merged microscopy images for the PTSA-bound microfibers were in accordance with the PTSA quenching data obtained (Fig. 2(c)-(j)). As shown in the images, an increase in the PTSA fluorescence intensities was noted for the microfibers from 0 h to 2.5 h. However, post 2.5 h, a decrease in fluorescence intensity of the PTSA-bound microfibers was noted. The results obtained from the images were in congruence with the data obtained benchtop spectrofluorometer and portable photometer. We thus considered a contact time of 2 h for further experiments. The microfiber detection rate determined from our study was quite comparable to the detection rate reported by the team of Lv et al., 2019. As per their published report, 54 particles/g (dry weight) microplastics would be detected, when stained using Safranine T, fluorescein isophosphate, Nile red, based on thermal expansion and contraction property. We obtained a detection rate of 27 ± 5.5 microfibers/mL which was equivalent to 62 particles/g of microfibers (subjected to variations based on the type of microfibers and length of the microfibers). This justified the applicability of the process for the real-time detection of microfibers in an aqueous environment using a portable photometer.

3.3. Effect of polymer variants

The type of polymer variant could be a vital attribute in the PTSA binding. Various fluorescence emission peaks and intensity values as a function of PTSA binding to four different pristine polymer variants namely, polyethylene, polypropylene, polyester, and cellulose are represented in Fig. 3(a)-(b). As per the data, fluorescence quenching was noted to be of a similar range in the case of sample microfibers, polyethylene, and polypropylene (Fig. 3(c), (e), (g)). However, polyester and cellulose were not found to significantly bind PTSA (Fig. 3(d), (f)). Cellulose is not commonly considered a microplastic, but rather an anthropogenic material (depending on the level of processing). So, an inability to analyze is not necessarily a downside. A one-sample *t*-test and Wilcoxon signed-rank test was performed for statistically analyzing the data (*p*-values noted to be 0.0054 and 0.0156 respectively). The p-values obtained confirmed the significance of the data when compared among the groups. An FT-IR analysis confirmed the specificity of the polymers towards PTSA via relevant changes in transmittance (%) values and peak shifts. The interactions between PTSA and microfibers have been discussed above (section 3.1).

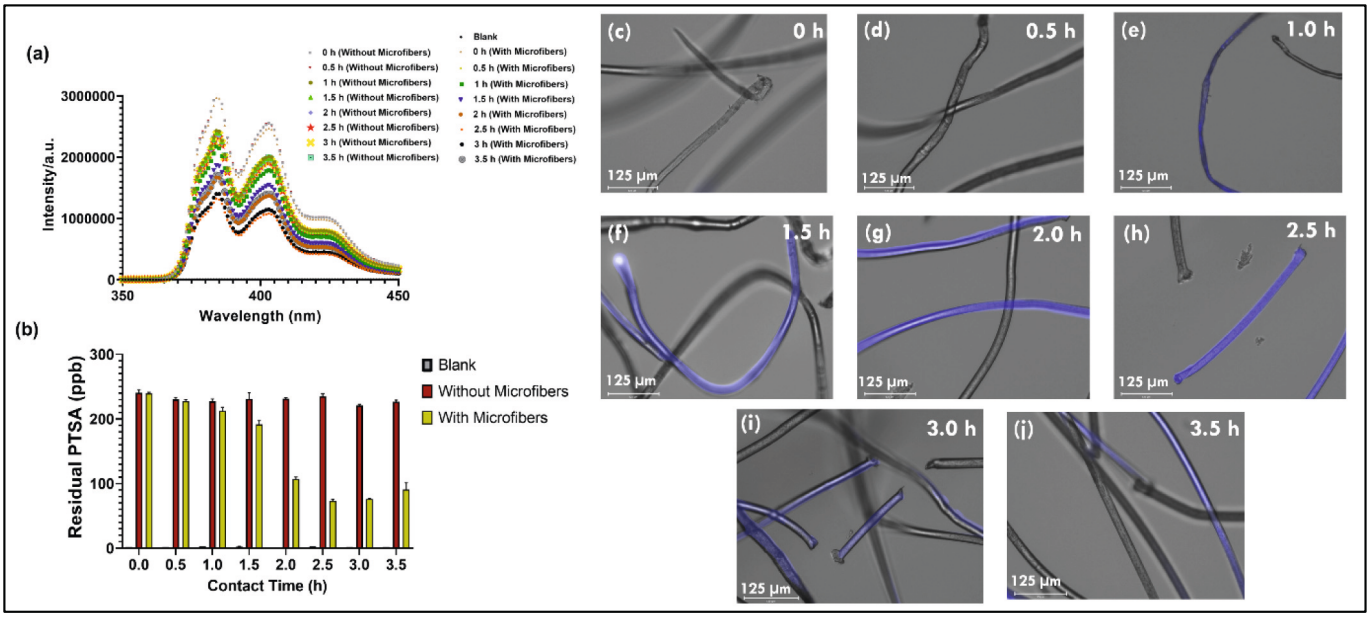

Fig. 2. Effect of varying contact time on PTSA binding to synthetic microfibers*[1] (a) fluorescence emission spectra (b) residual PTSA (ppb) values (c)-(j) merged bright field-fluorescence images.

*[1]The experiments were conducted in a 25 mL of AFW aqueous environment, at a temperature of 20 °C. pH value was measured to be 7.3 ± 0.47. The shaking speed was maintained at 150 rpm.

Statistical analyses were performed using a two-way ANOVA model. The *p*-values of the row factor (with and without microfibers) and column factor (different contact time values) were noted to be <0.0001

Microfiber count was noted as 13 ± 1.5 fibers/mL.

Average lengths of the fibers were noted to be 1073.6 ± 378.3 µm.

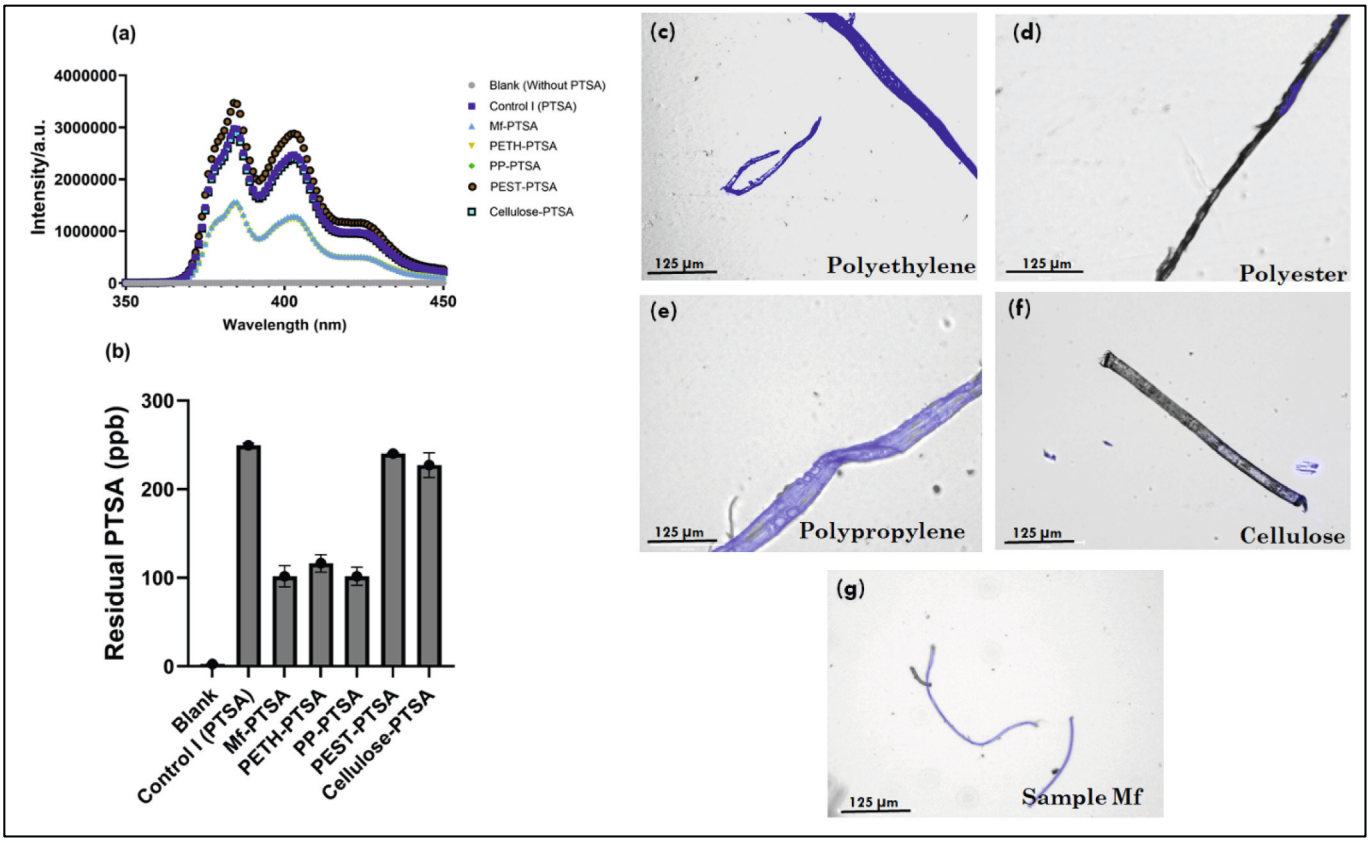

Fig. 3. PTSA quenching studies on microfibers of different polymeric variants (a) fluorescence emission spectra (b) residual PTSA (ppb) values (c)-(g) merged bright field-fluorescence images.
*The experiments were conducted in a 25 mL of AFW aqueous environment, at a temperature of 20 °C, contact time of 2 h, stirring rate of 150 rpm.
*One sample *t*-test and Wilcoxon signed rank test suggested significance in the variation of data
*The microfibers lengths as calculated using an Image J software tool: polyethylene: 537 ± 36.1 µm; polyester: 408 ± 12.7 µm; polypropylene: 664 ± 38.5 µm; Cellulose: 173 ± 36.7 µm; Sample microfibers: 352 ± 4.6 µm.
*The microfiber count was noted to be as follows: polyethylene: 11 ± 1.4 counts/mL; polyester: 12.5 ± 2.1 counts/mL; polypropylene: 8.3 ± 4.2 counts/mL; Cellulose: 18 ± 4.2counts/mL; Sample microfibers: 10 ± 0.7 counts/mL.

3.4. Effect of PTSA dosage

The PTSA dye dosage range considered was 0–1.31 nanomoles which was equivalent to the residual PTSA values of 2.3 ± 0.6 ppb – 259.3 ± 14.3 ppb (as obtained from the portable photometer MD-640). Both benchtop spectrofluorometer and portable photometer showed significant levels of PTSA quenching at all respective dye dosage values (Supplementary Fig. S9(a)-(b)). However, the optimum range for PTSA dosage could not be determined from the data obtained from benchtop and portable equipment set-ups. We, therefore, employed a fluorescence microscope to gain further insights into the same. The images were carefully obtained to contain at least 5 microfibers in a frame (Supplementary Fig. S9(c)-(j)). The PTSA dye binding was estimated in terms of the number of dyed microfibers to total number of microfibers considered in a frame. At a PTSA dosage of 0.102 nmoles, nil PTSA binding was noted, whereas, at a PTSA dye dosage of 0.307 nmoles, 2 out of 5 microfibers could bind the dye. Further, at PTSA dosage values of 0.610 nmoles and 0.822 nmoles, 5 or more microfibers exhibited fluorescence due to PTSA binding. The results suggested that the optimum dosage of PTSA could be maintained at a range of 0.6–0.8 nmoles to favour the applicability for microfiber detection in real environment.

3.5. Effect of external agents

The presence of external agents could cause interference in microplastic detection. In our study we have considered two insoluble (sand and chitin) and two soluble agents (zinc chloride and sodium chloride). The insoluble agents have been chosen based on their abundance along the coastlines. As shown in Supplementary Fig. S10(a)-(b), the quenching effect of chitin was slightly higher than sand, which could be attributed to the respective functional moieties on chitin. Samples A, B, and C comprised binary and ternary combinations of microfibers, sand, and chitin. No significant variations in PTSA quenching were noted when the respective insoluble external agents interacted with PTSA. However, the PTSA fluorescence intensities of insoluble external agents were comparatively lesser when compared to that of the synthetic microfibers (Supplementary Fig. S10(c)-(d)). The fluorescence emission peaks and residual PTSA concentration values are presented in Supplementary Fig. S10(a)-(b). Three different controls I, II, and III were chosen to assess any PTSA quenching by sand and chitin. As compared to controls I, II, and III, a significant reduction in the residual PTSA (ppb) was noted for samples A (43.2 % reduction), B (47.9 % reduction), and C (38.3 % reduction). The results obtained from the PTSA quenching studies and microscopy suggested low levels of interference by the external agents.

Zinc chloride is a chemical compound popularly used for microplastic extraction and is thus considered in the proposed study as a soluble external agent. Experiments were conducted in artificial freshwater (AFW) and artificial seawater (ASW) environments (containing 30 g/L NaCl dissolved in AFW aqueous media equivalent to 30 ppt). Based on the literature survey, a concentration range of 0–2.5 g/L for $ZnCl_2$ was chosen for our study (Rodrigues et al., 2020). As shown in

Fig. S11 (a)-(b), maximum quenching of PTSA was noted at nil dosage of $ZnCl_2$. At a dosage of 1.5 g/L, $ZnCl_2$ was found to interfere with the PTSA quenching by microfibers. This phenomenon could be attributed to the interference due to positively charged Zn^{2+} ions and their interaction with the sulfonate moieties of the PTSA dye molecules. Fluorescence images showed reduced levels of dye binding at a $ZnCl_2$ dosage of 1.5 g/L onwards (Fig. S11(c)-(h)). The PTSA quenching and the fluorescence intensities of the PTSA-bound microfibers were also assessed in an ASW aqueous environment. Interestingly, we found that the presence of sodium chloride resulted in an increase in the fluorescence intensity. As shown in Fig. S12(a)-(f), the fluorescence intensity of the PTSA bound microfibers was noticeably higher in group D (microfibers interacted with PTSA in an ASW environment) as compared to groups A, B, and C. In this regard, it would be worthy to mention the contribution of Liu et al. (2019), who reported an enhancement of fluorescence of dye bound to regenerated cellulose fabrics, in the presence of NaCl (Liu et al., 2019). Followed by the fluorescence intensities of group D, group A exhibited a significant level of PTSA fluorescence intensities. In the case of group B and group C, although the microfibers exhibited some levels of fluorescence intensities, however, compared to groups A and D, the intensities were suppressed due to $ZnCl_2$ interference. Supportive evidence was provided by the fluorescence emission spectra and photometer values (Fig. S11(a)-(b) and S12(a)-(b)). Appropriate controls were considered for the ease of comparison between the treatment groups with and without microfibers. The comparisons were made between control I-group A; control II-group B, control III-group C and control IV-group D, respectively. The levels of PTSA quenching were comparatively lesser when compared with groups A and B. Thus, we could infer that zinc chloride posed an interference in PTSA quenching by synthetic microfibers. However, the above results showed that although chloride could pose an interference in the process, however, compounds such as NaCl could significantly boost its fluorescence properties.

PTSA binding onto the synthetic microfibers along with mixed shapes was carried out under AFW and ASW aqueous environments (Supplementary Fig. S13(a)-(h)). Merged bright field-fluorescent images showed improved fluorescence of PTSA-bound fibers in an ASW environment as compared to that of an AFW environment (S13(e), (f), (g), (h)).

Further, the PTSA-based fluorescence detection technique was performed on real water samples collected from two different locations in the UK namely, Kirkstall, Leeds (River Aire as a freshwater source) and Sandsend village area, North Yorkshire region (as estuarine water and sea water sources. These were characterized and tabulated (Table S2). Merged bright field-fluorescence images showed that PTSA-bound microfibers exhibited higher fluorescence intensities in a natural seawater aqueous environment (SW) as compared to the intensities in estuarine and freshwater environments (Fig. 4 (a)-(c)). The results of PTSA quenching were depicted by the graphical analyses as shown in Fig. 4(d)-(e). PTSA quenching by the synthetic microfibers was similar in the case of all three types of aqueous environments, however, some variation in the fluorescence intensities of the PTSA-bound microfibers could be noted when a fluorescence microscope was employed. Thus, the Lovibond portable photometer could be used as a microplastic detection tool under aqueous environments.

3.6. Toxicity effects on Artemia salina

Toxic impacts of microfibers, PTSA, and PTSA-bound microfibers on brine shrimps (*Artemia salina*) were depicted in terms of Kaplan Maier plot and swimming competencies (Supplementary Fig. S14–S15, Tables S3–S4, section 2.3). In case of treatment group, A, the survival decreased to 40 % by day 4. However, for treatment groups B and C, the shrimps survived for 3 and 2 days respectively. This could be due to the dual impact of two foreign substances. Changes in behavioral properties were indicated in terms of swimming competencies. Initial exposure of the shrimps to microfibers reduced the swimming competencies from 85 % to 66 %, however, no significant changes in the swimming competencies were noted in the case of shrimps exposed to dye and dye-bound microfibers. However, after a period of 48 h exposure, a linear decrease in the swimming competencies was noted in the case of shrimps exposed to treatment groups A (60 %), B (52 %), and C (0 %) (videos provided). The combinatorial effects of microfibers and PTSA were found to exhibit a lethal effect at 48 h at which nil swimming competency was noted. The results suggested developing a suitable mitigation strategy for the dye post-detection. In our study, we have adopted a two-step mitigation strategy namely (i) dye recovery and (ii) sunlight-mediated degradation.

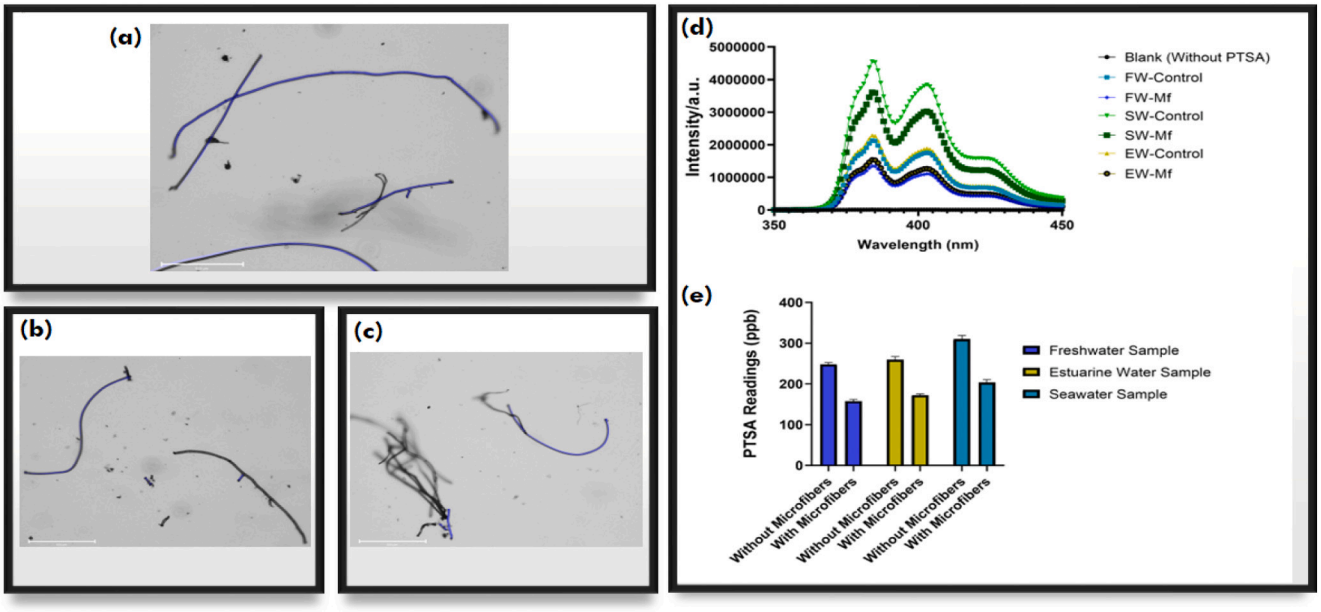

Fig. 4. PTSA based detection of microfibers spiked in different aqueous environments namely (a) seawater (b) estuarine water and (c) freshwater (d)-(e) PTSA quenching shown as fluorescence emission spectra and residual PTSA values (the characteristics of water samples have been provided in Supplementary Table S2).

3.7. Dye recovery studies

The recovery of microfiber-bound PTSA was studied by performing detailed experimentation on the interaction between xanthan gum (an anionic biopolymer) and PTSA-bound microfibers. The interaction study was conducted with a major aim to recover the dye bound to the microfibers. We reasoned that the use of xanthan gum biopolymer to recover the bound dye based on their interaction with the PTSA dye and their respective viscosity profiles (Supplementary section 2.4.1; supplementary Figs. S16 and S17).

The dosage of xanthan gum was chosen at a concentration range of 0.1 g/L-0.4 g/L based on the viscosity profiles. A confocal microscopy imaging of the PTSA-bound microfibers and the respective interactions with low and high-dosage xanthan gum has been represented in Fig. 5 (a)-(c)). The hypothesis has been represented in a schematic illustration (Fig. 5(d)). When a lower dosage of xanthan gum was added to PTSA-bound microfibers, it resulted in the release of PTSA dye to the surrounding aqueous environment (indicated by the reduced blue intensity on the microfibers in Fig. 5(b) as compared to bright blue intensity in Fig. 5(a)). This resulted in an increase in fluorescence intensity values in the surrounding aqueous environment (Supplementary Fig. S18(c)-(d)). The comparisons on the fluorescence intensity values of PTSA in the surrounding aqueous solution was made with respect to a control (various xanthan gum dosages interacted with PTSA dye) (Supplementary Fig. S18(a)-(b)). This could be attributed to the competitive binding of xanthan gum due to its anionic nature. However, a higher dosage range of 0.3–0.4 g/L resulted in a decrease in PTSA fluorescence intensity. This could be attributed to the PTSA quenching by excess of xanthan gum present in the solution or bound to the microfibers (indicated by the presence of slight blue intensity in the xanthan gum bound to the microfibers in Fig. 5(c) indicated by the red arrow). FT-IR analyses of the samples were performed to further assess the interactions between xanthan gum, microfiber and PTSA (Supplementary Fig. S19). Changes in peak transmission (%) were noted in the wavenumber range of 2946–2840 cm^{-1} which could be attributed to -CH_2 and -CH stretching vibrations of the microfibers. The appearance of a peak at 1646 cm^{-1} confirmed the binding of xanthan gum to the microfibers (Alharthi et al., 2023). A characteristic peak (due to the C—S bond) appeared at 1172 cm^{-1} for PTSA-bound microfibers and PTSA-bound microfibers interacted with xanthan gum (at a dosage of 0.1 g/L). However, a peak disappearance was noted when xanthan gum was added at a dosage value (0.4 g/L). This could be attributed to the PTSA quenching by the presence of excess xanthan gum.

The recovered PTSA was further subjected to sunlight-mediated photodegradation. The sunlight-mediated degradation of the recovered PTSA dye has been explained in Supplementary Section 2.5 and Fig. S20 (a)-(c). The fluorescence intensity values for the dye were noted to be reduced by 50 % on exposure to sunlight (114 ± 7.5 ppb) on day 20 and further, no fluorescence intensity was noted (<3 ppb) on day 40.

4. Conclusion

Microfibers released from surgical face masks (composed of polyethylene and polypropylene) were considered as a microplastic model. The microfibers could effectively bind the fluorescent 1,3,6,8 pyrene tetra sulfonate dye (PTSA) and changes in the fluorescence intensities could be monitored using a portable pocket photometer (MD-640, Lovibond Tintometer group). Optimal binding of microfibres to PTSA was noted at pH range: 4.0–9.0; contact time-2 h and temperature range:20 °C–60 °C. The dye was noted to selectively bind to the microfibers based on their polymeric nature. Among the four standards considered, polyethylene and polypropylene were found to exhibit a higher dye-binding capacity. The presence of a soluble external agent (Zinc Chloride) at a dosage beyond 1 g/L reduced the binding of PTSA to microfibers. However, the presence of sodium chloride resulted in an increase in the overall fluorescence intensities. Insoluble external agents such as chitin and sand did not significantly affect the PTSA binding.

Risk assessment studies were performed using *Artemia salina* as a model organism. The presence of both microfibers and PTSA resulted in maximum mortality at the end of 48 h. Thus, we designed a sustainable two-step mitigation strategy was designed which included dye recovery followed by sunlight-mediated degradation. Post-detection of microfibers, and dye recovery was performed using xanthan gum as a natural anionic polysaccharide. Binding of xanthan gum to the microfibers resulted in the release of the dye molecules from microfibers, which was indicated in terms of the increase in fluorescence intensities. A low dosage of 0.1–0.2 % *w/v* could release the PTSA to the surrounding aqueous environment, however, a higher dosage of 0.3–0.4 % w/v resulted in PTSA quenching due to excess of biopolymer in the suspension. Post-release from the microfibers, PTSA could be effectively degraded on exposure to sunlight for a period of 40 days.

The data obtained from our work could have a broader impact on the scientific community and could be relevant to academics and industry experts working in the broad arena of clean water, who are specifically interested in developing cost-effective solutions for effective detection and biomonitoring of emerging pollutants.

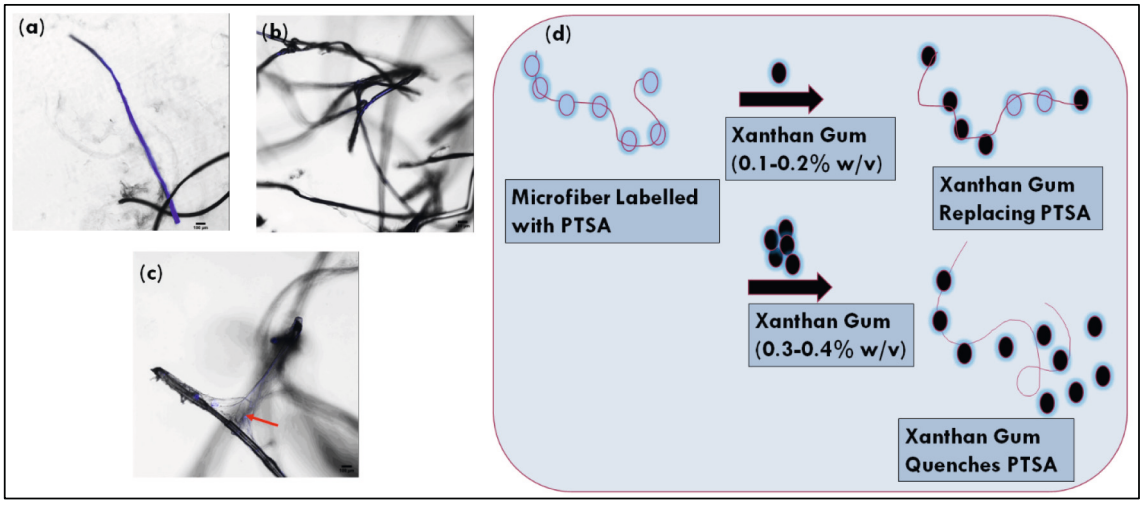

Fig. 5. Interactions between xanthan gum and PTSA bound synthetic microfibers explained using (a)-(c) confocal microscopy* and (d) schematic illustration
*The confocal laser scanning microscopy images were obtained at a magnification of 10× and processed using a FIJI tool. The bioimaging equipment (LSM880 + Airyscan Inverted Confocal Microscope).

CRediT authorship contribution statement

Dr. Devlina Das Pramanik: Conceptualization, Plan of Work, Investigation, Formal analyses, Manuscript- Writing, Review & Editing; Prof. Paul Kay: Supervision, Review & Editing; Prof. Francisco M. Goycoolea: Hosting and Supervision; Resources, Review & Editing.

Declaration of competing interest

The authors declare that they have no known competing financial interests or personal relationships that could have appeared to influence the work reported in this paper.

Data availability

Data will be made available on request.

Acknowledgement

The work has been funded by the European Commission (H2020-MSCA-IF-2019) (Marie Skłodowska-Curie Individual Fellowships, Type of action: MSCA-IF-EF-ST (Standard European Fellowships) Proposal number: 897736). The research has been carried out at the School of Food Science and Nutrition (Hosted and Supervised by Professor Francisco M. Goycoolea), in collaboration with the School of Geography (Hosted and Supervised by Professor Paul Kay), University of Leeds, United Kingdom. We would also like to acknowledge the contribution of the dedicated technical teams of School of Food Science and Nutrition, School of Geography, Bioimaging and FACS facility (Faculty of Biological Sciences and the School of Chemistry, University of Leeds, UK. We like to acknowledge the contribution of Robert Wills, Product Specialist, Agilent Technologies, UK, for their extensive support provided. We would also like to acknowledge the contribution of the technical team from Drop Test Kits (DTK Water), UK for providing prompt support with apparatus delivery and technical guidance.

Appendix A. Supplementary data

Supplementary data to this article can be found online at https://doi.org/10.1016/j.scitotenv.2023.168144.

References

Alharthi, F.A., Alshammari, R.H., Hasan, I., 2023. Synthesis of xanthan gum anchored α-Fe2O3 bionanocomposite material for remediation of Pb (II) contaminated aquatic system. Polymers (Basel) 15 (5), 1134. https://doi.org/10.3390/polym15051134.

Alvim, C.B., Bes-Piá, M.A., Mendoza-Roca, J.A., Alonso-Molina, J.L., 2023. Identification of microfibers in drinking water with Nile Red. Limitations and strengths. J. Environ. Chem. Eng. 11 (3), 109697 https://doi.org/10.1016/j.jece.2023.109697.

Anastopoulos, I., Pashalidis, 2021. Single-use surgical face masks, as a potential source of microplastics: do they act as pollutant carriers? J. Mol. Liq. 326, 115247 https://doi.org/10.1016/j.molliq.2020.115247.

Asamoah, B.O., Kanyathare, B., Roussey, M., Peiponen, K.E., 2019. A prototype of a portable optical sensor for the detection of transparent and translucent microplastics in freshwater. Chemosphere 231, 161–167. https://doi.org/10.1016/j.chemosphere.2019.05.114.

Asamoah, B.O., Uurasjärvi, E., Räty, J., Koistinen, A., Roussey, M., Peiponen, K.E., 2021. Towards the development of portable and in situ optical devices for detection of micro and nanoplastics in water: a review on the current status. Polymers (Basel) 13 (5), 730. https://doi.org/10.3390/polym13050730.

Brown, E., MacDonald, A., Allen, S., Allen, D., 2023. The potential for a plastic recycling facility to release microplastic pollution and possible filtration remediation effectiveness. J. Hazard. Mater. Adv. 10, 100309 https://doi.org/10.1016/j.hazadv.2023.100309.

Cabrejos-Cardeña, U., De-la-Torre, G.E., Dobaradaran, S., Rangabhashiyam, S., 2023. An ecotoxicological perspective of microplastics released by face masks. J. Hazard. Mater. 443, Part B, 130273 https://doi.org/10.1016/j.jhazmat.2022.130273.

Chen, L., Hu, B., Zhang, J., Zhang, J., Huang, S., Ren, P., Zou, Y., Ding, F., Liu, X., Li, H., 2019. A facile synthesis of 1,3,6,8-pyrenesulfonic acid tetrasodium salt as a hydrosoluble fluorescent ink for anti-counterfeiting applications. RSC Adv. 9, 476–481. https://doi.org/10.1039/C8RA09106D.

Chen, H.L., Gibbins, C.N., Selvam, S.B., Ting, K.N., 2021. Spatio-temporal variation of microplastic along a rural to urban transition in a tropical river. Environ. Pollut. 289, 117895 https://doi.org/10.1016/j.envpol.2021.117895.

Dowarah, K., Patchaiyappan, A., Thirunavukkarasu, C., Jayakumar, S., Devipriya, S.P., 2020. Quantification of microplastics using Nile Red in two bivalve species Perna viridis and Meretrix meretrix from three estuaries in Pondicherry, India and microplastic uptake by local communities through bivalve diet. Mar. Pollut. Bull. 153, 110982 https://doi.org/10.1016/j.marpolbul.2020.110982.

de Guzman, M.K., Andjelković, M., Jovanović, V., Jung, J., Kim, J., Dailey, L.A., Rajković, A., Meulenaer, B.D., Veličković, T.C., 2022. Comparative profiling and exposure assessment of microplastics in differently sized Manila clams from South Korea by μFTIR and Nile Red staining. Mar. Pollut. Bull. 181, 113846 https://doi.org/10.1016/j.marpolbul.2022.113846.

Idowu, G.A., Olalemi, A.O., Aiyesanmi, A.F., 2023. Environmental impacts of covid-19 pandemic: release of microplastics, organic contaminants and trace metals from face masks under ambient environmental conditions. Environ. Res. 217, 114956 https://doi.org/10.1016/j.envres.2022.114956.

Jiao, L., Zhang, M., Li, H., 2020. Preparation of 1, 3, 6, 8-pyrenesulfonic acid tetrasodium salt dye-doped silica nanoparticles and their application in water-based anti-counterfeit ink. Materials 13 (18), 4074. https://doi.org/10.3390/ma13184074.

Liu, H., Lu, M., Pan, F., Ning, X., Ming, J., 2019. Influence of fluorescent dyes for dyeing of regenerated cellulose fabric. Text. Res. J. 90 (11−12), 1385–1395. https://doi.org/10.1177/0040517519892915.

Lv, Lulu, Qu, J., Yu, Z., Chen, D., Zhou, C., Hong, P., Sun, S., Li, C., 2019. A simple method for detecting and quantifying microplastics utilizing fluorescent dyes - Safranine T, fluorescein isophosphate, Nile red based on thermal expansion and contraction property. Environ. Pollut. 255, Part 2, 113283 https://doi.org/10.1016/j.envpol.2019.113283.

Meyers, N., Catarino, A.I., Declercq, A.M., Brenan, A., Devriese, L., Vandegehuchte, M., Witte, B.D., Janssen, C., Everaert, G., 2022. Microplastic detection and identification by Nile red staining: towards a semi-automated, cost- and time-effective technique. Sci. Total Environ. 823, 153441 https://doi.org/10.1016/j.scitotenv.2022.153441.

Nalbone, L., Panebianco, A., Giarratana, F., Russell, M., 2021. Nile red staining for detecting microplastics in biota: preliminary evidence. Mar. Pollut. Bull. 172, 112888 https://doi.org/10.1016/j.marpolbul.2021.112888.

Nel, H.A., Chetwynd, A.J., Kelleher, L., Lynch, I., Mansfield, I., Margenat, H., Onoja, S., Oppenheimer, P.G., Smith, G.H.S., Krause, S., 2021. Detection limits are central to improve reporting standards when using Nile red for microplastic quantification. Chemosphere 263, 127953. https://doi.org/10.1016/j.chemosphere.2020.127953.

Park, D.H., Oh, S.B., Hong, S.C., 2022. Fluorescent illumination of microplastics in water utilizing a combination of dye/surfactant and quenching techniques. Polymers 14 (15), 3084. https://doi.org/10.3390/polym14153084.

Pramanik, D.D., Lei, S., Kay, P., Goycoolea, F.M., 2023. Investigating on the toxicity and bio-magnification potential of synthetic glitters on *Artemia salina*. Mar. Pollut. Bull. 190, 114828 https://doi.org/10.1016/j.marpolbul.2023.114828.

Prata, J.C., da Costa, J., Fernandes, A.J.S., da Costa, F.M., Duarte, A.C., Rocha-Santos, T., 2021. Selection of microplastics by Nile Red staining increases environmental sample throughput by micro-Raman spectroscopy. Sci. Total Environ. 783, 146979 https://doi.org/10.1016/j.scitotenv.2021.146979.

Rodrigues, M.O., Gonçalves, A.M.M., Gonçalves, F.J.M., Abrantes, N., 2020. Improving cost-efficiency for MPs density separation by zinc chloride reuse. MethodsX 7, 100785. https://doi.org/10.1016/j.mex.2020.100785.

Shim, W.J., Song, Y.K., Hong, S.H., Jang, M., 2016. Identification and quantification of microplastics using Nile Red staining. Mar. Pollut. Bull. 113 (1–2), 469–476. https://doi.org/10.1016/j.marpolbul.2016.10.049.